

Fully Nonlinear Electromagnetic Gyrokinetic Computations

B. Scott

Max-Planck-IPP, EURATOM Association, Garching, Germany

Gyrokinetic computation with particle-in-cell [1, 2, 3, 4] and phase space grid [5, 6, 7, 8] models has been very current for tokamak core turbulence, following developments in the modern version of the theory from late 1980s [9, 10] to present [11]. The theory is for “total-f” (or “full-f”) models carrying the entire distribution function as a dependent variable, while most of the applications are for “delta-f” models studying small-amplitude microturbulence on a prescribed background. Recently, total-f models are also emerging [12, 13]. The delta-f version with collisions and non-ballooning coordinates is also being used with edge turbulence [14]. Various efforts for total-f computation of edge turbulence are still in development. One of the major hurdles is the necessity found by electromagnetic gyrofluid global models to carry the entire MHD equilibrium including neoclassical flows as part of the dependent variables [15].

An essential part of this is the demonstration of the global geodesic Alfvén oscillation as part of the dynamics. In an artificial initial state, a perfectly one-dimensional (radial) dependence of all dependent variables (the “zonal” components) results in a diamagnetic current with a finite divergence caused by geodesic curvature. In the absence of a parallel current, the polarisation current provides divergence balance. This represents a temporal rise in the initially absent ExB vorticity. The resulting parallel electric field then drives a parallel current, in turn whose divergence acts as a restoring force. These pieces combine in an Alfvén oscillation between the $\sin \theta$ electrostatic potential and $\cos \theta$ parallel current. Dissipation of the oscillation leaves the parallel current in its equilibrium state: the Pfirsch-Schlüter current. Ampere’s law gives the parallel $\cos \theta$ magnetic potential representing the Shafranov shift. All of the aforementioned components are axisymmetric. Ordinarily, this would be a neglected component, but the turbulence drives “zonal flows” (the ExB flows resulting from the zonal potential) through Reynolds and Maxwell stresses which also knock the currents slightly out of equilibrium. Dissipation of these forms a significant dissipation channel for zonal flow energy, and even local delta-f models have to treat these processes [16]. The added difficulty for any total-f model is that the zonal diamagnetic current now results from the dependent variable, which includes the pressure profile. Changes in the profile lead to changes in the current balances, which must include the total Pfirsch-Schlüter current. Even if large amplitude oscillations are avoided by slowly increasing the pressure gradient to its prescribed level during an initialisation, the physics of the global geodesic Alfvén oscillation remains, and the numerics must be able to treat it.

The total-f gyrokinetic equation results from a Lagrangian which describes the particles and also the self consistent field potentials [17, 18]. The polarisation and induction equations for these potentials also result from the same Lagrangian, as does the global energy which is conserved. The Lagrangian is derived using Lie transform techniques; we follow the version used by Hahm [9] but with the parallel magnetic potential also present [10]. The polarisation is somewhat simplified, retaining the dominant ExB energy contribution. In this work the emphasis is on the equilibrium, so gyroaveraging is neglected and long-wavelength forms are used in the polarisation terms. The Lagrangian is

$$L = \sum_{\text{sp}} \int d\Lambda \left[\left(\frac{e}{c} \mathbf{A} + p_z \mathbf{b} \right) \cdot \dot{\mathbf{R}} + \frac{mc}{e} \dot{\vartheta} - H \right] f - \int dV \frac{B_{\perp}^2}{8\pi} \quad (1)$$

where the Hamiltonian, generalised potential, and squared ExB velocity are

$$H = m \frac{U^2}{2} + \mu B + e\phi_G \quad \phi_G = \phi - \frac{m v_E^2}{e} \quad v_E^2 = \frac{c^2}{B^2} |\nabla_{\perp} \phi|^2 \quad (2)$$

and the parallel velocity functional and perturbed magnetic field strength are given by

$$U = \frac{1}{m} \left(p_z - \frac{e}{c} A_{\parallel} \right) \quad B_{\perp}^2 = |\nabla_{\perp} A_{\parallel}|^2 \quad (3)$$

with dV and dW the space and velocity space volume elements, and $d\Lambda = dV dW$ is the phase space volume element. The sum is over species and m and e are the mass and charge of each species. The resulting gyrokinetic equation is

$$B_{\parallel}^* \frac{\partial f}{\partial t} + \nabla H \cdot \frac{c \mathbf{F}}{e B} \cdot \nabla f + \mathbf{B}^* \cdot \left(\frac{\partial H}{\partial p_z} \nabla f - \frac{\partial f}{\partial p_z} \nabla H \right) = C(f) \quad (4)$$

where $\mathbf{F} = (\nabla \mathbf{A}) - (\nabla \mathbf{A})^T$ and $\mathbf{B}^* = \mathbf{B} - p_z (c/e) \nabla \cdot (\mathbf{F}/B)$ and $B_{\parallel}^* = \mathbf{b} \cdot \mathbf{B}^*$. Here we approximate $\mathbf{F} \approx (RB/I) \mathbf{F}_0$ with $I = R_0 B_0$ a constant and $\nabla \cdot \mathbf{F}_0 = 0$, so that $B_{\parallel}^* = B$. We assume arbitrarily weak collisionality so that the collision operator C consists of hyperdiffusion in p_z and s (actual collisions are to be implemented later). The spatial coordinates $\{x, y, s\}$ describe a unit-Jacobian Hamada global field-aligned system [19], so that $dV = dx dy ds$. The velocity space grid is on $\{p_z, \mu\}$ so that $dW = 2\pi m^{-2} B dp_z d\mu$. The self consistent field equations resulting from variation of L with respect to ϕ and A_{\parallel} are

$$\sum_{\text{sp}} \int dW \left[e f + \nabla \cdot \frac{f m c^2}{B^2} \nabla_{\perp} \phi \right] = 0 \quad \nabla_{\perp}^2 A_{\parallel} + \frac{4\pi}{c} \sum_{\text{sp}} \int dW e U f = 0 \quad (5)$$

giving quasineutral polarisation and shear-Alfvén induction, respectively (note here that U in the integral also involves A_{\parallel}). Eqs. (4–5) are solved using 4th-order Arakawa Jacobians [20] and a Karniadakis time step [21], and standard tri-diagonal methods for the field potentials.

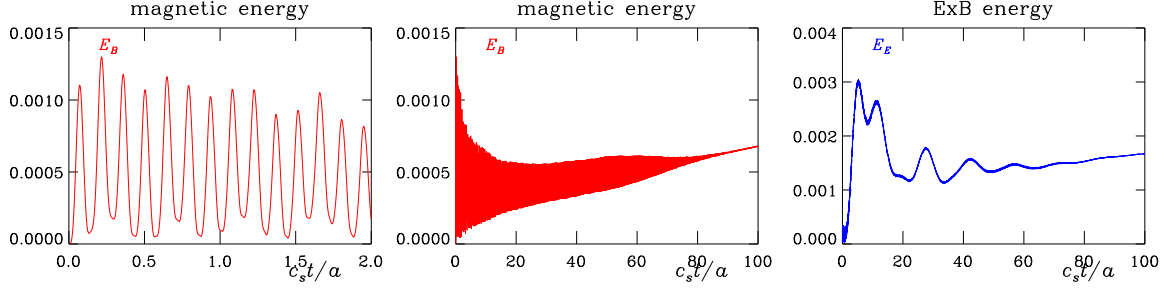


Figure 1: (left) Evolution of the magnetic energy E_B during the initial phases of the global geodesic Alfvén oscillation. (center) On a longer time scale, the Alfvén oscillation decays through electron Landau damping. (right) The ExB energy E_E exhibits the geodesic acoustic oscillation, which decays through ion Landau damping. The field energies grow following changes in the ion pressure profile.

In the computations described here only the axisymmetric dynamics is considered hence $\partial/\partial y = 0$, with x and s representing enclosed flux surface volume and unit-cycle poloidal angle. The domain is $0.85 < r_a < 0.99$ with $r_a = (x/x_{\max})^{1/2}$. The coordinate geometry is circular concentric, with the Shafranov shift occurring in the dependent variables, and $|\nabla_{\perp}\phi|^2$ is approximated by $g^{xx}(\partial\phi/\partial x)^2$. The standard case is initialised using a Maxwellian $f_0(n, T)$ and profile function $p_f = (1/6) \sin[\pi(r_0 - r_a)/0.14]$, with $n = 3 \times 10^{13} \text{ cm}^{-3} \exp[p_f(x)]$ and $T = 200 \text{ eV} \exp[3 p_f(x)]$ set equally with both species, with $r_0 = 0.92$ and masses m_e for electrons and $M_D = 3670 m_e$ for deuterium ions. The major radius was $R = R_0 + r_a a_0 \cos \theta$ with $R_0 = 165 \text{ cm}$ and minor radius $a_0 = 50 \text{ cm}$, and the magnetic field was set such that $BR = B_0 R_0$ with $B_0 = 2.5 \text{ T}$ and $q = 1.5 + 2.5 r_a^2$. The global geodesic Alfvén oscillation proceeds naturally, with time evolution of the magnetic energy given in Fig. 1. On a slower time scale, the ExB energy exhibits geodesic acoustic oscillations, which damp quickest for lower r_a hence lower q , with the oscillations at the outer boundary lasting about twice as long. The energy pieces are respectively given by

$$E_f + E_E + E_B = \sum_{\text{sp}} \int d\Lambda \left[\left(m \frac{U^2}{2} + \mu B \right) + m \frac{v_E^2}{2} \right] f + \int dV \frac{B_{\perp}^2}{8\pi} \quad (6)$$

The collisionless Landau damping dissipates all the oscillations, and the equilibrium into which f_e and f_i fall has the expected neoclassical structure, as shown in Fig. 2. The zonal profile $\phi(r)$ follows the expected force balance relation, with $n_e e \nabla_r \phi + \nabla_r p_i$ approximately vanishing. In addition (not shown), the parallel current is in its expected state with the Pfirsch-Schlüter $\cos \theta$ piece dominant. This state stops evolving when the ion distribution function stops readjusting (quantitative analysis of this requires collisions). Further development of this model will add collisions and turbulence, for a comprehensive description of the tokamak edge. One

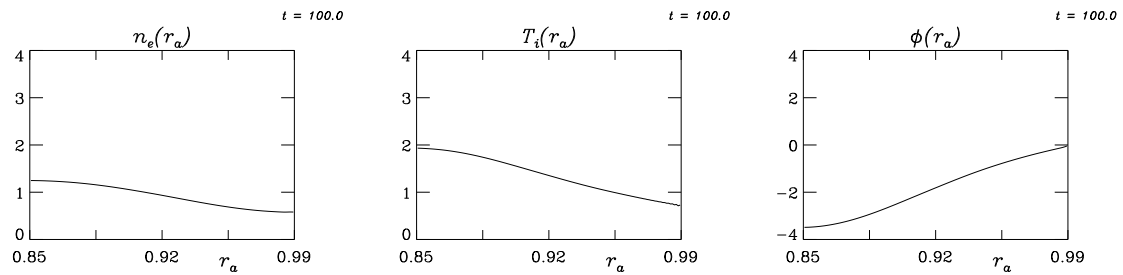


Figure 2: After all the oscillations have decayed away the zonal potential profile is in equilibrium with the ion pressure, given by the density and temperature

outstanding issue is the need to dynamically align the grid to the flux surfaces [15]. It is not yet clear how to do this in a total-f setting where A_{\parallel} appears nonlinearly in the trapping dynamics.

References

- [1] Lin Z, Hahm T S, Lee W W, Tang W M and White R B 1998 *Science* **281** 1835–1837
- [2] Hatzky R, T M Tran A K, Kleiber R and Allfrey S J 2002 *Phys. Plasmas* **9** 898
- [3] Parker S E, Chen Y, Wan W, Cohen B I and Nevins W M 2004 *Phys. Plasmas* **11** 2594
- [4] Idomura Y, Ida M, Tokuda S and Villard L 2007 *J. Comput. Phys.* **226** 244–262
- [5] Kotschenreuther M, Rewoldt G and Tang W M 1995 *Comput. Phys. Comm.* **88** 128
- [6] Jenko F, Dorland W, Kotschenreuther M and Rogers B N 2000 *Phys. Plasmas* **7** 1904
- [7] Candy J and Waltz R E 2006 *Phys. Plasmas* **13** 032310
- [8] Watanabe T H and Sugama H 2006 *Nucl. Fusion* **46** 24–32
- [9] Hahm T S 1988 *Phys. Fluids* **31** 2670
- [10] Hahm T S, Lee W W and Brizard A 1988 *Phys. Fluids* **31** 1940
- [11] Brizard A and Hahm T S 2007 *Rev. Mod. Phys.* **79** 421–468
- [12] Heikkinen J A, Henriksson S, Janhunen S, Kiviniemi T P and Ogando F 2006 *Contrib. Plasma Phys.* **46** 490–495
- [13] Grandgirard V, Sarazin Y, Angelino P, Bottino A, Crouseilles N, Darinet G, Dif-Pradalier G, Garbet X, Ghendrih P, Joliet S, Latu G, Sonnendrücker E and Villard L 2007 *Plasma Phys. Contr. Fusion* **49** B173–B182
- [14] Scott B 2006 *Plasma Phys. Contr. Fusion* **48** A387–A392
- [15] Scott B 2006 *Contrib. Plasma Phys.* **46** 714–725
- [16] Scott B 2005 *New J. Phys.* **7** 92
- [17] Brizard A 2000 *Phys. Plasmas* **7** 4816
- [18] Sugama H 2000 *Phys. Plasmas* **7** 466
- [19] Scott B 2001 *Phys. Plasmas* **8** 447–458
- [20] Arakawa A 1966 *J. Comput. Phys.* **1** 119 repr. vol 135 (1997) 103
- [21] Karniadakis G E, Israeli M and Orszag S A 1991 *J. Comput. Phys.* **97** 414